Abiotic sugar synthesis from CO_2 electrolysis

Stefano Cestellos-Blanco[1,2^], Sheena Louisia[3,4^], Michael B. Ross[3,5], Yifan Li[3,4], Tyler C. Detomasi[3], Jessica N. Cestellos Spradlin[3], Daniel K. Nomura[3,6], and Peidong Yang[1,2,3,4,7*]

[1] Department of Materials Science and Engineering, University of California, Berkeley, Berkeley, CA, USA
[2] Center for the Utilization of Biological Engineering in Space (CUBES), University of California, Berkeley, Berkeley, CA, USA
[3] Department of Chemistry, University of California, Berkeley, Berkeley, CA, USA
[4] Chemical Sciences Division, Lawrence Berkeley National Laboratory, Berkeley, CA, USA
[5] Current affiliation: Department of Chemistry, University of Massachusetts, Lowell, Lowell MA, USA
[6] Department of Nutritional Science and Toxicology, University of California, Berkeley, Berkeley, CA, USA
[7] Kavli Energy Nanosciences Institute, Berkeley, CA, USA

^ These authors contributed equally.
* Author to whom correspondence should be addressed: p_yang@berkeley.edu.

ABSTRACT

CO_2 valorization is aimed at converting waste CO_2 to value-added products. While steady progress has been achieved through diverse catalytic strategies, including CO_2 electrosynthesis, CO_2 thermocatalysis, and biological CO_2 fixation, each of these approaches have distinct limitations. Inorganic catalysts only enable synthesis beyond C_2 and C_3 products with poor selectivity and with a high energy requirement. Meanwhile, although biological organisms can selectively produce complex products from CO_2, their slow autotrophic metabolism limits their industrial feasibility. Here, we present an abiotic approach leveraging electrochemical and thermochemical catalysis to complete the conversion of CO_2 to life-sustaining carbohydrate sugars akin to photosynthesis. CO_2 was electrochemically converted to glycolaldehyde and formaldehyde using copper nanoparticles and boron-doped diamond cathodes, respectively. CO_2-derived glycolaldehyde then served as the key autocatalyst for the formose reaction, where glycolaldehyde and formaldehyde combined in the presence of an alkaline earth metal catalyst to form a variety of C_4 - C_8 sugars, including glucose. In turn, these sugars were used as a feedstock for fast-growing and genetically modifiable *Escherichia coli*. Altogether, we have assembled a platform that pushes the boundaries of product complexity achievable from CO_2 conversion while demonstrating CO_2 integration into life-sustaining sugars.

INTRODUCTION

As an abundant and inexpensive waste product, CO_2 is an attractive feedstock to produce functional chemicals and materials.[1–3] CO_2 is also a prime target for *in situ* resource utilization on Mars to enable crewed deep space exploration.[4–6] Various inorganic CO_2 catalysts operated either thermo- or electrochemically have been developed but products have categorically been limited to C_{1-3} products with low selectvity.[7] Thermocatalytic platforms usually have high capital costs and require elevated temperature and pressure reactors to produce carbon products mostly through CO_2 hydrogenation and methanation.[8] Electrochemical CO_2 reduction platforms can be powered modularly by any electricity source and thus be sustained by renewable solar or wind energy sources, offering a promising way to close the loop of the carbon cycle.[9] Although catalytic optimization has been successful for the generation of the main 2 e^- reduction products, CO and $HCOO^-$, the formation of higher-order products has remained a challenge.[10–12] Cu remains the only element that displays a high turnover rate towards multi-carbon (C_{2+}) products.[13,14] However, limited progress has been made to boost its selectivity towards C_{2+} molecules due to the complexity of favoring one out of the many possible reaction pathways. Additionally, CO_2 has rarely been converted into molecules larger than three carbons due to the difficulty for one surface to successively facilitate multiple steps with distinct energy requirements.[15–19] CO_2 bioelectrosynthesis employing autotrophic bacteria as biocatalysts is a complementary approach to the purely inorganic catalyst-mediated electrochemical CO_2RR affording high selectivity to C_{2+} products. [20,21] However, CO_2 turnover rates for autotrophic bacteria are orders of magnitude lower than those from heterogeneous electrochemical CO_2 reduction due to their sluggish autotrophic metabolism, and the requirement to maintain biocompatible conditions within the electrochemical set-up. sit

The ability to leverage the independent strengths of inorganically catalyzed CO_2 reduction and biocatalysis would be transformative, enabling scalable CO_2 reduction with selective production of multi-carbons. Recently, the National Aeronautics and Space Administration (NASA) launched a Centennial Challenge focused on converting CO_2 to carbohydrate sugars.[22] These are to be employed as a high energy feedstock for fast growing and genetically modifiable bacteria like *Escherichia coli* (*E. coli*) enabling large scale chemical and material biomanufacturing. Therefore, the conversion of CO_2 to sugars would enable the selective biogeneration of a vast array of products.

On Earth, phototrophs convert CO_2 to polycarbohydrates establishing the first link in the food chain. However, to date, the abiotic conversion of CO_2 to sugars has not been reported. Here we show (**Figure 1)** that, by combining electrochemical CO_2 reduction with formose chemistry, we can use CO_2-derived glycolaldehyde as an autocatalyst to synthesize sugars in sufficient quantities to sustain a living

heterotrophic organism. We used a Cu nanoparticle (NP) ensemble electrocatalyst well-suited for the CO_2 electroconversion to glycolaldehyde.[23,24] Other than Cu-based CO_2RR, there is no clear one-pot CO_2 to glycolaldehyde conversion process.[25,26] We directly combine the glycolaldehyde-containing electrolyte with formaldehyde under formose reaction conditions to synthesize C_4-C_8 sugars, including glucose. These sugars were then used as a feedstock for an *E. coli* culture. Altogether, we demonstrate a synthetic route to integrate CO_2 into the production of life-sustaining sugars.

RESULTS AND DISCUSSION

CO_2 electrochemical reduction to aldehyde precursors

The electrochemical reduction of CO_2 on Cu catalysts yields more than 16 different products with aldehydes often contributing to less than 5% of the total faradaic efficiency (FE).[18] The formation of surface bound CO (*CO) intermediates and subsequent C-C coupling are both necessary steps for the mechanistic pathway leading to the formation of aldehydes and further reduced C_{2+} products (**Fig. 2a**). However, after C-C coupling, aldehydes are expected to be further reduced which is likely the reason for their overall lower efficiency.[27–29] Consequently, catalysts that have been reported with high FE for C_{2+} products, and especially for C_{2+} oxygenates, are more likely to produce an intermediate species like glycolaldehyde. The Cu NP ensemble previously reported in our group (**Fig. 2b**) is therefore an ideal candidate to optimize the production of glycolaldehyde due to its high intrinsic activity for CO_2-to-C_{2+} conversion at low overpotential (i.e., partial current density per surface Cu atom 7-fold greater than traditional Cu foil at -0.80 V vs RHE).[23,24] The catalytic properties of this Cu NP ensemble towards glycolaldehyde specifically sits in a favorable range both in terms of selectivity (FE) and activity (current density) when compared to other Cu-based catalysts (**Fig. S1 and S2**). We evaluated the performance of the Cu NP ensemble across different applied potentials to maximize the rate of CO_2-to-glycolaldehyde production. We identified the peak production to reach 12 μg/hour at -0.80 V vs RHE (**Fig. 2c**). An increase or decrease in the overpotential is likely more favorable to the reduction of produced aldehydes or the hydrogen evolution reaction (HER), respectively. Indeed, the peak production of glycolaldehyde occurs at a more positive potential than ethylene and ethanol further suggesting that a too negative applied potential will further reduce any produced aldehydes (**Fig. S3**).

Given the optimal applied potential, we then investigated how to further maximize the concentration of glycolaldehyde. The CO_2RR activity of the Cu NP ensemble remains steady after hours of operation as demonstrated by the stable current density and product distribution monitored by gas

chromatography (GC) (**Fig. 2d and S4**). However, the concentration of aldehyde begins to plateau after 5 hours of electrolysis (**Fig. S5**). The interrupted accumulation of aldehyde is likely due to their propensity towards further reduction to alcohol or alkene over time.[27–29] As a result, we considered 4 hours CO_2RR adequate to consistently obtain a high enough concentration of glycolaldehyde.

Despite our optimization of the CO_2 electroconversion to glycolaldehyde, the reaction is inherently limited, and the FE of this process has rarely been improved beyond 2-3%. Consequently, we explored ways to convert CO_2 to another relevant reactant for the production of sugars: formaldehyde. Traditionally, formaldehyde is derived from syngas or methanol through well-established industrial synthetic processes.[32,38] Nakata *et al*. have presented a promising electrocatalytic avenue to convert CO_2 to formaldehyde with a FE of up to 65% using a boron-doped diamond (BDD) electrode.[30] Inspired by this demonstration, we combined previous insights obtained from CO_2 electroreduction on BDD to evaluate its potential for the aqueous production of formaldehyde (**Discussion S1 and Fig. 2b)**. However, using the same reaction conditions as reported by Nakata et al., we did not produce formaldehyde at a comparable FE, and the reaction was principally dominated by HER (**Fig. 2e and Fig. S6**).[30] Future work will require further investigation of the catalyst synthesis to enhance the selectivity. In addition, the high reactivity of this molecule exacerbated both under reducing conditions and in the presence of hydroxyl anions will require adjusted reactor and operation design to maximize the reaction turnover.

Sugar syntheses using the formose reaction

The formose reaction was established by Aleksandr Butlerov in 1861 though it received renewed attention in the 1950's and 60's principally led by Ronald Breslow and Alvin Weiss.[31–33] The reaction is catalyzed by an alkaline metal ion (e.g., Ca^{2+}) under mild heating and alkaline conditions. Condensations and tautomerizations of reactive intermediates convert aldehyde starting products into a heterogeneous mixture of sugars through a cyclical polymerization-like process (**Fig. 3a**).[31] Though various formose catalysts have been employed, we used Ca as it is a low-cost and non-toxic catalyst, which is significant if the sugars are to be used as a feedstock in a bioprocess.[34–36]

Having demonstrated CO_2RR for the generation of glycolaldehyde and formaldehyde, we sought to verify the formose reaction conditions for the conversion of glycolaldehyde and formaldehyde to sugars. We initially optimized the formose reaction with non-CO_2 derived standard samples of glycolaldehyde and formaldehyde. While the formose reaction has been thought to start as the aldol condensation of two formaldehyde molecules to form glycolaldehyde, such direct dimerization only occurs in very specific conditions (i.e., in the gas-phase or under gamma-irradiation) and has been appraised in the literature as "chemically impossible" in the absence of glycolaldehyde in aqueous solutions.[37–39] Thus the Cannizzaro

disproportionation of formaldehyde dominates in an alkaline environment converting formaldehyde to methanol and formic acid instead of sugars.[31,40] As a result, we confirmed experimentally that formaldehyde alone with $Ca(OH)_2$ yields only methanol and formic acid **(Figs. 3a and S7)**. The formose process can be initiated by adding glycolaldehyde, thus shortening the induction period and suppressing the competing Cannizzaro reaction.[38] Glycolaldehyde autocatalytically initiates the formose reaction cycle, in which formaldehyde condenses to a second molecule of glycolaldehyde. The autocatalytic cycle occurs at a much faster rate producing more glycolaldehyde which also reacts with other intermediates to form higher order sugars. Sugars can arise from aldol condensations involving glycolaldehyde as the active methylene component and another aldehyde as the carbonyl component.[31] Glycolaldehyde, even in trace quantities, is an essential autocatalyst for the formation of sugars. We verified that glycolaldehyde alone produces sugars confirming a sugar formation pathway through glycolaldehyde **(Figs. 3a and S7)**. Therefore, electrochemical CO_2RR-derived glycolaldehyde (e-CO_2Glyc) is a necessary element autocatalyzing CO_2-derived sugar (CO_2Sugar) production.

The formose reaction conditions were optimized to yield the highest quantity of biological feedstock products such as glucose (**Fig. 3**). High-performance anion exchange chromatography with pulsed amperometric detection (HPAEC-PAD) was used for the separation and detection of a variety of carbohydrates of comparable weights (**Methods and Fig. 3**).[41] Unlike other analytical techniques, the separation allows for the identification of structurally similar carbohydrates (i.e., glucose vs fructose) (**Fig. S8**).

As a wide range of temperatures has been reported to enable the formose reaction, we tested a range from 45 to 85°C in 10°C increments (**Fig. 3b**).[42] A minimum temperature of 55°C was required to activate the reaction. Furthermore, 65°C yielded a higher proportion of C5 sugars (63%), while 75°C yielded more C6 sugars (78%). The total of 2.6 μmol sugars obtained at 75°C further decreases to 0.66 μmol at 85°C, as sugars may decompose into tar at the elevated temperature. We further determined the required concentration of formaldehyde to drive the formose reaction (**Fig. 3c)**. The Cannizzaro reaction dominates at concentrations below 35 mM as higher formaldehyde concentrations are needed to provide a driving force for C-C bond formation.[32] We found that a concentration of 70 mM formaldehyde adequately serves to synthesize feedstock sugar products. We observed that formaldehyde concentrations starting at 140 mM do not adequately generate sugars. As has been previously described, this is caused by an insufficient concentration of insoluble $Ca(OH)_2$ present to catalyze the reaction.[43] Lastly, as the concentration of e-CO_2Glyc is low (~ 30 μM), it is essential to establish the minimum glycolaldehyde concentration necessary to autocatalyze the formose reaction. We determined this threshold concentration to be 1 μM as presented in **Figure 3d**. This is commensurate with glycolaldehyde provided by the CO_2RR. A higher total amount of sugars is obtained with higher glycolaldehyde concentrations (**Fig. 3d**). In summary, in the adapted

reaction conditions of 70 mM formaldehyde, 75°C and 10 μM glycolaldehyde among the biologically relevant sugars that we identified glucose is the major product (49%), followed by fructose (20%), ribose (17%), galactose (8%), and arabinose (5%).

CO_2 electrolysis products as sugar building blocks

After establishing the optimal conditions for the formose reaction, we tested whether e-CO_2RR-derived products could undergo the formose reaction. The as-obtained concentration of formaldehyde is too low to support the formose reaction as evidenced by **Figure 3c**. Formaldehyde can be obtained in high yields from CO_2 through industrially established high temperature and pressure hydrogenation of CO_2 to methanol and subsequent formox process.[44–46] Formaldehyde can also be concentrated through fractional distillation, which we attempted to partial success but are not presently able to sufficiently scale up (**Fig. S9**). The direct conversion of glycolaldehyde alone to sugars is another avenue enabled by the formose reaction, as glycolaldehyde alone enables sugar generation (**Fig. S7**). However, presently achievable e-CO_2Glyc concentration is too low to alone support the formose reaction (**Fig. S10**). As with formaldehyde, a high concentration of glycolaldehyde is required for sugar generation through the formose reaction (**Fig. S11**). As formaldehyde can be obtained industrially in high titers from CO_2 and there is no demonstrated CO_2-to-glycolaldehyde one-pot synthesis, we focused our efforts on e-CO_2Glyc as the essential formose autocatalyst. Hence, we demonstrate a proof-of-concept sugar generation from commercial formaldehyde (to be CO_2-derived) autocatalyzed by e-CO_2Glyc.

We used the unadulterated CO_2 electrolysis product stream as the glycolaldehyde source with our optimized formose reaction conditions for the conversion of formaldehyde to sugars. The high $KHCO_3$ concentration (0.1 M) in the electrolysis product mixture posed further obstacles. Firstly, the Ca^{2+} and CO_3^{2-} combine to form highly insoluble $CaCO_3$ which does not adequately catalyze the formose reaction. Secondly, $KHCO_3$ acts as a buffer that alters the optimal pH upon addition of the divalent metal catalyst. Thirdly, the high salinity of the reaction mixture complicates product characterization with mass spectrometry by suppressing ionization. Nonetheless, we were able to introduce sufficient $Ca(OH)_2$ for the reaction to proceed by adding excess $Ca(OH)_2$ 10 mM above the concentration of $KHCO_3$ and by carefully titrating the reaction mixture pH with NaOH/HCl to pH 11.

The use of the unadulterated CO_2 electrolysis product stream to produce CO_2Sugars presents another challenge with the introduction of a multitude of coexisting CO_2-derived molecules. The complexity of the reaction mixture complicates the analysis of CO_2Sugars. Therefore, unlike in the previous formose reaction optimizations, HPAEC-PAD measurements are in part affected by the high concentrations of other CO_2-derived products (e.g., ethanol, formate) and by the presence of HCO_3^- anions (**Fig. S12)**.

Fortunately, the spectral signature of sugars is easily distinguishable using ^{1}H-NMR. Specifically, the chemical shifts for carbohydrate protons are typically observed in the 3.5-5 ppm region while most of the other CO_2RR products are found in the 0-4 and >7 ppm region (**Fig. S13**). Therefore, the appearance of multiple peaks in this region was used as an initial indication for the formation of CO_2Sugars. With the Ca^{2+} catalyst concentration and pH optimization, ^{1}H-NMR results indicate that CO_2Sugars formation can be autocatalyzed by CO_2Glyc (**Fig. 4a**).

Beyond the sugar fingerprint identified by ^{1}H-NMR, we used electrospray ionization mass spectrometry (ESI-MS) to further determine the variety of CO_2Sugars.[47] As previously mentioned, the high salinity of our reaction containing K^+, Na^+, and Ca^{2+} poses an obstacle to ESI-MS analysis. Therefore, we separated our CO_2Sugars from the salty aqueous solution via liquid-liquid extraction by protecting their hydroxyl groups (benzylation), thus increasing their solubility in organic solvents (**Fig. S14)**. The derivatization of CO_2Sugars by benzylation and separation from the salty mixture allowed their characterization by ESI-MS. These measurements revealed a diverse mixture of fully and partially benzylated carbohydrates ranging from three to eight carbons (**Fig. 4b**).

Although powerful, ESI-MS analysis is limited to the identification of sugars of the same molecular weight. HPAEC-PAD remains the method of choice to distinguish multiple carbohydrates of similar compositions (i.e., glucose from galactose or fructose). The high baseline tailing effect observed in the chromatogram of CO_2Sugars likely results from the saturation of the column due to the high concentrations of HCO_3^- present as buffer (**Fig. S12 and S16**). Nevertheless, carbohydrates in the reaction mixture are still distinguishable during HPAEC-PAD measurements. Comparing the chromatograms of carbohydrate standards with the reaction mixture of CO_2Sugars confirms the presence of biologically relevant sugars such as glucose (**Fig. 4c)**. Further separation of the reaction mixture from HCO_3^- and other overlapping molecules will be required to improve the analysis of CO_2Sugars and enable quantification by HPAEC-PAD. Additionally, a more extensive survey of carbohydrate standards beyond those that are significant as biological feedstocks should be performed to complete the catalog of CO_2Sugars produced.

To highlight the broad applicability and reproducibility of employing e-CO_2Glyc as the autocatalyst in the formose reaction, we used e-CO_2Glyc obtained at varying CO_2RR conditions. We compared the CO_2Glyc generated at three successive potentials with the Cu NP ensemble and with Cu foil. The input e-CO_2Glyc concentration was normalized across the electrolytes before beginning the formose reaction. As demonstrated by the ^{1}H NMR and HPAEC-PAD spectra (**Fig. S15 and S16**) for the four different conditions, there is little difference in the ensuing CO_2Sugars. This confirms that the formose reaction is robustly adaptive to different CO_2RR conditions given sufficient CO_2Glyc.

E. coli cultures supported by CO_2-derived sugars

With biologically relevant sugars—ribose, galactose, fructose, arabinose, and glucose— in hand, we sought to use them to sustain bacterial growth. Glucose is the preferred source of carbon for *E. coli*; however, it can also metabolize a variety of other carbohydrates including many of those produced in the formose reaction.[48] We collected the products from the standard formose reaction and from CO_2Sugars and employed them directly as feed sources for *E. coli* cultures. We used minimal processing to prepare the formose sugars; briefly, we syringe filtered the solutions directly after the formose reaction to remove precipitates, crystallized the sugars via rotary evaporation which also removed cytotoxic components (e.g., methanol, ethanol), and added a commensurate amount (0.1% w/v) to M9 minimal bacterial medium (Table S2). The medium containing the formose sugars was syringe sterilized before inoculating with *E. coli*. Culture growth and biomass accumulation were assessed by optical density. Formose- and CO_2Sugars-fed cultures achieved maximum optical densities of ~0.26 and ~0.22, reaching stationary phases after 4.3 and 3.8 hours respectively (**Fig. 5a**). These optical density values correspond to nearly half of the maximum optical density of a control *E. coli*. culture provided with 0.1% pure glucose (**Fig. S17).** The optical density of the formose-fed *E. coli* culture is expectedly lower as the feed source consists of a mixture of sugars that may not be metabolizable or metabolized suboptimally when compared to pure glucose. Nevertheless, these results demonstrate that CO_2Sugars can sustain heterotrophic microorganisms in a raw form with little processing. This minimization of processing and separation steps that may be resource-prohibitive is especially valuable for industrial and extra-terrestrial applications. Furthermore, we verified that available CO_2Sugars present in minimal medium were consumed during bacterial growth. To establish this, we obtained ^{1}H-NMR spectra before and after the culturing period. As exhibited in **Figure 5c** the carbohydrate associated proton peaks mostly disappear after bacteria are grown in the medium. Finally, *E. coli* growth can be visually confirmed in the medium containing different sugars sources (**Fig. 5b**). In the future, we envision the production of CO_2Sugars could be coupled with a biomanufacturing platform to generate value-added products on demand.

When taken together, we demonstrate an approach to employ the outputs of CO_2 electrosynthesis to generate sugars. Our work invites the CO_2 electrocatalysis community to reconsider the processing value of so far overlooked by-products. Although minor, some of the building blocks present in the streamline of CO_2 electrolysis could be readily utilized for the construction of biologically-significant molecules. However, there remain several scale-up steps to be determined before achieving a catalytic turnover akin to biological processes. The electrochemical production of both glycolaldehyde and formaldehyde presented in our work is limited to the μM scale. To maximize these turnovers, catalyst development, electrochemical conditions, and setup designs will require further investigation. As an example, the

application of a flow cell design can be used to minimize the further reduction of produced glycolaldehyde. Further studies of the catalyst properties necessary to advance the CO_2 electroreduction to formaldehyde will be required to achieve the targeted activity. For the maximization of both aldehyde concentrations, an additional processing step of distillation should be considered. With such developments, we envision that this inorganic platform could rival photosynthesis in commercial sugar production and could mitigate CO_2-driven climate change. Overall, this proof of concept demonstrates how various catalytic systems can be tailored to facilitate CO_2 conversion to life-sustaining molecules, far beyond the hydrocarbons usually reported in the field of CO_2 electrocatalytic up-cycling.

MATERIALS AND METHODS

Electrochemical CO_2 reduction

7 nm Cu nanoparticles were synthesized as previously reported.[23] Boron-doped diamond (BDD) electrode (Electrode Kit Boron Doped Diamond, IKA) was rinsed with 20% HNO_3 and sonicated in DI water before use. All electrochemical measurements were carried in a custom-made H-cell consisting of two main compartments separated by a Selemion AMV anion exchange membrane (AEM). Ag/AgCl (WPI, 3 M KCl) was used as a reference electrode and a platinum wire was used as a counter electrode.

For glycolaldehyde production, 0.1 M $KHCO_3$ electrolyte was prepared by purging a 0.05 M K_2CO_3 (99.997% trace metal basis) solution with CO_2 overnight. Both the working and counter chambers were filled with 17 mL of the electrolyte and vigorous stirring was maintained in the working chamber. The input stream of CO_2 was humidified by being bubbled through DI water before being introduced into the cell. Before each measurement, the 17 mL catholyte was purged with 20 sccm CO_2 for 15-20 min until saturated.

Formaldehyde production was carried in various electrolytes including 0.1 M NaCl, 0.1 M $KHCO_3$, and 0.1 M $HClO_4$. The same procedure as for the CO_2-to-glycolaldehyde reaction described above was executed.

All electrode potentials measured against 3 M KCl Ag/AgCl reference were converted to the RHE scale using E (vs RHE) = E (vs Ag/AgCl) + 0.210 V + 0.0591 × pH. For all electrochemical experiments, 84% of ohmic loss was compensated by the potentiostat (Biologic) in real-time and the remaining 16% was manually post-corrected. Glycolaldehyde concentration was determined using quantitative NMR (qNMR) (Bruker AV-600) following. Dimethyl sulfoxide is used as an internal standard and an aliquot of the solution of interest prepared in D_2O. Solvent presaturation technique is implemented to suppress the water peak.

The concentration of gases produced throughout electrolysis was measured using a gas chromatograph (SRI GC) connected at the outlet of the cell. Gas chromatograph is equipped with a molecular sieve 13X (1/8" × 6') and hayesep D (1/8" × 6') column with Ar flowing as a carrier gas. Sample for gas chromatography was collected at 20-minute intervals and the separated gas products were analyzed by a thermal conductivity detector (for H_2) and a flame ionization detector (for CO and hydrocarbons). Quantification of the products was performed with conversion factors derived from the standard calibration gases and the concentration of gas measured was further converted to partial current density.

A formaldehyde detection assay (Sigma-Aldrich MAK131) was employed to quantify formaldehyde concentrations. Briefly, formaldehyde is derivatized with acetoacetanilide in the presence of ammonia yielding a fluorescent product with excitation and emission wavelengths at 370 nm and 470 nm, respectively. The fluorescent signal proportional to formaldehyde concentration was read using a Biotek Synergy LX Multi-Mode microplate reader.

Faradaic efficiencies (FE) were calculated from the amount of charge passed to produce each product divided by the total charge passed at a specific time (gas) or during the overall run (liquid).

Formose reaction

The formose reaction was performed as described in previous literature.[34,36] Initial reagents were paraformaldehyde, glycolaldehyde dimer, and $Ca(OH)_2$ (Sigma Aldrich). Commercial paraformaldehyde was suspended in distilled water, heated to 70°C, and refluxed under alkaline conditions to depolymerize, producing a homogeneous, colorless solution. Glycolaldehyde and $Ca(OH)_2$ were dissolved in distilled water. The total reaction volume was typically 3 mL with 10 mM $Ca(OH)_2$, with the concentrations of formaldehyde and glycolaldehyde as well as the temperature dependent on desired experimental conditions. The reactions were carried out for 75 minutes and then quickly cooled down to room temperature. Upon completion, the samples exhibited the characteristic bright yellow color of the formose reaction. For CO_2-

derived formose reaction, the CO_2RR electrolyte was used directly without any processing. For example, for a 3 mL reaction volume, 1.5 mL of CO_2RR electrolyte with 30 μM glycolaldehyde was combined with an equivalent volume of distilled water. $Ca(OH)_2$ and formaldehyde were added to concentrations of 60 and 70 mM, respectively. The reaction was maintained at 75°C for 75 minutes. The pH was titrated with 1 M NaOH/HCl to 11.

Product and material characterization

^{1}H-NMR

The liquid products accumulated during CO_2 electrolysis and the sugars produced during the formose reaction are analyzed by quantitative NMR (qNMR) (Bruker AV-600) following the same procedure. Dimethyl sulfoxide is used as an internal standard and an aliquot of the solution of interest prepared in D_2O. Solvent presaturation technique is implemented to suppress the water peak.

Mass spectrometry

The produced carbohydrates are benzylated to ensure their separation from their salty matrix post-formose reaction.[49] The aqueous sample is mixed with $NaOH/K_2CO_3$ (1/4, w/w), benzene, isopropanol, tetrabutylammonium hydrogen sulfate, benzyl chloride, and DMSO. The solution is then vigorously stirred using a stir bar at room temperature for 4 hours. Subsequently, the mixture is worked up using cyclohexane, washed with water, and dried over Na_2SO_4. The benzylated carbohydrates were then injected into an electrospray ionization mass spectrometer (ESI-MS) for mass analysis.

HPAEC-PAD

The completed reactions were analyzed by high-performance anion exchange chromatography with pulsed amperometic detection on a Dionex ICS-5000. The samples were run on a CarboPac™ PA20 IC Column using a 0.4 mL/min isocratic gradient as follows: with 10 mM NaOH for 30 min, 100 mM NaOH for 5 min, and 10 mM NaOH for 5 min. A gold electrode in carbohydrate quad potential mode was employed as the detector. Upon injection, the elution is carried with 10 mM NaOH for 30 min, 100 mM NaOH for 5 min, and 10 mM NaOH for 5 min. Runs were compared to standards of (2-6 carbon) biologically relevant sugars: arabinose, glucose, ribose, fructose, acetaldehyde as well as formaldehyde were employed to identify peaks in the trace.

SEM

Cu nanoparticle coated and BDD electrodes were directly imaged by SEM at 5 keV (Ultra 55-FESEM).

Cell culture

XL1-blue *E. coli* cells were obtained from the Berkeley-QB3 MacroLab. *E. coli* stock stored at -80°C, was inoculated in Lysogeny Broth (**Table S1**) and incubated at 37°C in three consecutive cultures to remove any cryoprotectant. The formose reaction solution was filtered to remove precipitates and the products were recovered using a rotary evaporator. The experiment appropriate mass of bulk formose sugars (0-0.1% (w/v)) was added to the M9 minimal medium and syringe filtered to sterilize. The cells were then inoculated in M9 minimal medium (**Table S2**) supplemented with glucose or formose sugars. *E. coli* growth curves were acquired in a Tecan M1000 plate reader in a 48-well plate for 24 hours at 37°C under continuous orbital shaking.

REFERENCES

1. Liu, Q., Wu, L., Jackstell, R. & Beller, M. Using carbon dioxide as a building block in organic synthesis. *Nature Communications 2015 6:1* **6**, 1–15 (2015).
2. Alain Goeppert, Miklos Czaun, Prakash, G. K. S. & A. Olah, G. Air as the renewable carbon source of the future: an overview of CO 2 capture from the atmosphere. *Energy & Environmental Science* **5**, 7833–7853 (2012).
3. Hepburn, C. *et al.* The technological and economic prospects for CO2 utilization and removal. *Nature 2019 575:7781* **575**, 87–97 (2019).
4. Curtis V. Manning, Christopher P. McKay & Kevin J. Zahnle. Thick and thin models of the evolution of carbon dioxide on Mars. *Icarus* **180**, 38–59 (2006).
5. Muscatello, A. C. & Santiago-Maldonado, E. Mars In Situ Resource Utilization Technology Evaluation. doi:10.2514/6.2012-360.
6. Berliner, A. J. *et al.* Towards a Biomanufactory on Mars. *Frontiers in Astronomy and Space Sciences* **0**, 120 (2021).
7. Tackett, B. M., Gomez, E. & Chen, J. G. Net reduction of CO2 via its thermocatalytic and electrocatalytic transformation reactions in standard and hybrid processes. *Nature Catalysis 2019 2:5* **2**, 381–386 (2019).
8. Li, W. *et al.* A short review of recent advances in CO2 hydrogenation to hydrocarbons over heterogeneous catalysts. *RSC Advances* **8**, 7651–7669 (2018).
9. Jiang, Z., Xiao, T., Kuznetsov, V. L. & Edwards, P. P. Turning carbon dioxide into fuel. *Philosophical Transactions of the Royal Society A: Mathematical, Physical and Engineering Sciences* **368**, 3343–3364 (2010).
10. Oloman, C. & Li, H. Electrochemical Processing of Carbon Dioxide. *ChemSusChem* **1**, 385–391 (2008).
11. Feaster, J. T. *et al.* Understanding Selectivity for the Electrochemical Reduction of Carbon Dioxide to Formic Acid and Carbon Monoxide on Metal Electrodes. *ACS Catalysis* **7**, 4822–4827 (2017).
12. Philips, M. F., Gruter, G.-J. M., Koper, M. T. M. & Schouten, K. J. P. Optimizing the Electrochemical Reduction of CO2 to Formate: A State-of-the-Art Analysis. *ACS Sustainable Chemistry & Engineering* **8**, 15430–15444 (2020).
13. Hori, Y., Kikuchi, K. & Suzuki, S. Production of CO and CH4 in Electrochemical Reduction of CO2 at Metal Electrodes in Aqueous Hydrogencarbonate Solution. *Chemistry Letters* 1695–1698 (1985).
14. Jitaru, M., Lowy, D. A., Toma, M., Toma, B. C. & Oniciu, L. Electrochemical reduction of carbon dioxide on flat metallic cathodes. *Journal of Applied Electrochemistry 1997 27:8* **27**, 875–889 (1997).
15. Zheng, Y. *et al.* Understanding the Roadmap for Electrochemical Reduction of CO2 to Multi-Carbon Oxygenates and Hydrocarbons on Copper-Based Catalysts. *Journal of the American Chemical Society* **141**, 7646–7659 (2019).
16. Ross, M. B. *et al.* Designing materials for electrochemical carbon dioxide recycling. *Nature Catalysis* **2**, 648–658 (2019).
17. Xue, Y., Guo, Y., Cui, H. & Zhou, Z. Catalyst Design for Electrochemical Reduction of CO2 to Multicarbon Products. *Small Methods* **5**, 2100736 (2021).

18. P. Kuhl, K., R. Cave, E., N. Abram, D. & F. Jaramillo, T. New insights into the electrochemical reduction of carbon dioxide on metallic copper surfaces. *Energy & Environmental Science* **5**, 7050–7059 (2012).
19. Rui, L. *et al.* Electrochemical Reduction of Carbon Dioxide to 1-Butanol on Oxide-Derived Copper. *Angewandte Chemie* **132**, 21258–21265 (2020).
20. Chen, H., Dong, F. & Minteer, S. D. The progress and outlook of bioelectrocatalysis for the production of chemicals, fuels and materials. *Nature Catalysis* vol. 3 225–244 (2020).
21. Cestellos-Blanco, S., Zhang, H., Kim, J. M., Shen, Y. xiao & Yang, P. Photosynthetic semiconductor biohybrids for solar-driven biocatalysis. *Nature Catalysis* vol. 3 245–255 (2020).
22. Harbaugh, J. *NASA Awards $750,000 in Competition to Convert CO2 into Sugar*. http://www.nasa.gov/directorates/spacetech/centennial_challenges/75K-awarded-in-competition-to-convert-carbon-dioxide-into-sugar.html (2021).
23. Kim, D., Kley, C. S., Li, Y. & Yang, P. Copper nanoparticle ensembles for selective electroreduction of CO2 to C2–C3 products. *Proceedings of the National Academy of Sciences of the United States of America* **114**, 10560–10565 (2017).
24. Li, Y. *et al.* Electrochemically scrambled nanocrystals are catalytically active for CO2-to-multicarbons. *Proceedings of the National Academy of Sciences* **117**, 9194–9201 (2020).
25. Mohan, D., Pittman Jr., C. U. & Steele, P. H. Pyrolysis of Wood/Biomass for Bio-oil: A Critical Review. *Energy and Fuels* **20**, 848–889 (2006).
26. Schandel, C. B., Høj, M., Osmundsen, C. M., Jensen, A. D. & Taarning, E. Thermal Cracking of Sugars for the Production of Glycolaldehyde and Other Small Oxygenates. *ChemSusChem* **13**, 688–692 (2020).
27. Charnay, B. P., Cui, Z., Marx, M. A., Palazzo, J. & Co, A. C. Insights into the CO2 Reduction Pathway through the Electrolysis of Aldehydes on Copper. *ACS Catalysis* **11**, 3867–3876 (2021).
28. Clark, E. L. & Bell, A. T. Direct Observation of the Local Reaction Environment during the Electrochemical Reduction of CO2. *Journal of the American Chemical Society* **140**, 7012–7020 (2018).
29. Löffler, M., Khanipour, P., Kulyk, N., Mayrhofer, K. J. J. & Katsounaros, I. Insights into Liquid Product Formation during Carbon Dioxide Reduction on Copper and Oxide-Derived Copper from Quantitative Real-Time Measurements. *ACS Catalysis* **10**, 6735–6740 (2020).
30. Nakata, K., Ozaki, T., Terashima, C., Fujishima, A. & Einaga, Y. High-Yield Electrochemical Production of Formaldehyde from CO2 and Seawater. *Angewandte Chemie International Edition* **53**, 871–874 (2014).
31. Breslow, R. On the mechanism of the formose reaction. *Tetrahedron Letters* **1**, 22–26 (1959).
32. Mizuno, T. & Weiss, A. H. Synthesis and utilization of formose sugars. *Advances in Carbohydrate Chemistry and Biochemistry* **29**, 173–227 (1974).
33. Butlerow, A. Bildung einer zuckerartigen Substanz durch Synthese. *Justus Liebigs Annalen der Chemie* **120**, 295–298 (1861).
34. Lambert, J. B., Gurusamy-Thangavelu, S. A. & Ma, K. The silicate-mediated formose reaction: Bottom-up synthesis of sugar silicates. *Science* **327**, 984–986 (2010).
35. Pallmann, S. *et al.* Schreibersite: An effective catalyst in the formose reaction network. *New Journal of Physics* **20**, 55003 (2018).
36. Appayee, C. & Breslow, R. Deuterium studies reveal a new mechanism for the formose reaction involving hydride shifts. *Journal of the American Chemical Society* **136**, 3720–3723 (2014).

37. Eckhardt, A. K., Linden, M. M., Wende, R. C., Bernhardt, B. & Schreiner, P. R. Gas-phase sugar formation using hydroxymethylene as the reactive formaldehyde isomer. *Nature Chemistry* (2018) doi:10.1038/s41557-018-0128-2.
38. Khomenko, T. I. *et al.* Homogeneously catalyzed formaldehyde condensation to carbohydrates: IV. Alkaline earth hydroxide catalysts used with glycolaldehyde co-catalyst. *Journal of Catalysis* **45**, 356–366 (1976).
39. Irie Setsuko. Selective Formose Reaction Initiated By Photo- And γ-Irradiation. *Chemistry Letters* **13**, 2153–2156 (1984).
40. Tambawala, H. & Weiss, A. H. Homogeneously catalyzed formaldehyde condensation to carbohydrates: II. Instabilities and Cannizzaro effects. *Journal of Catalysis* **26**, 388–400 (1972).
41. Ball, G. F. M. The application of HPLC to the determination of low molecular weight sugars and polyhydric alcohols in foods: A review. *Food Chemistry* **35**, 117–152 (1990).
42. Omran, A., Menor-Salvan, C., Springsteen, G. & Pasek, M. The Messy Alkaline Formose Reaction and Its Link to Metabolism. *Life 2020, Vol. 10, Page 125* **10**, 125 (2020).
43. Yoshihiro, S., Takashi, F., Chikahiro, S. & Teruo, M. Formose Reactions. III. Evaluation of Various Factors Affecting the Formose Reaction. *Bulletin of the Chemical Society of Japan* **50**, 1527–1531 (1977).
44. Heim, L. E., Konnerth, H. & Prechtl, M. H. G. Future perspectives for formaldehyde: Pathways for reductive synthesis and energy storage. *Green Chemistry* vol. 19 2347–2355 (2017).
45. Soares, A. P. V., Portela, M. F. & Kiennemann, A. Methanol Selective Oxidation to Formaldehyde over Iron-Molybdate Catalysts. *http://dx.doi.org/10.1081/CR-200049088* **47**, 125–174 (2007).
46. Millar, G. J. & Collins, M. Industrial Production of Formaldehyde Using Polycrystalline Silver Catalyst. *Industrial and Engineering Chemistry Research* **56**, 9247–9265 (2017).
47. Shen, X. & Perreault, H. Characterization of carbohydrates using a combination of derivatization, high-performance liquid chromatography and mass spectrometry. *Journal of Chromatography A* **811**, 47–59 (1998).
48. Lendenmann, U. & Egli, T. Is Escherichia coli growing in glucose-limited chemostat culture able to utilize other sugars without lag? *Microbiology* **141**, 71–78 (1995).
49. Szeja, W., Fokt, I. & Grynkiewicz, G. Benzylation of sugar polyols by means of the PTC method. *Recueil des Travaux Chimiques des Pays-Bas* **108**, 224–226 (1989).

ACKNOWLEDGMENTS

This work was supported by an award from the National Aeronautics and Space Administration (NASA) under the Centennial Challenges competition program. The authors thank the judges and competition administrators for their feedback. This work was also supported by the Director, Office of Science, Office of Basic Energy Sciences, Chemical Sciences, Geosciences, & Biosciences Division, of the US Department of Energy under Contract DE-AC02-05CH11231, FWP CH030201 (Catalysis Research Program) and by NASA, under grant number NNX17AJ31G. ICP-OES was supported by the Microanalytical Facility, College of Chemistry, UC Berkeley. We thank the staff at UC Berkeley's NMR facility in the College of Chemistry (CoC-NMR) for spectroscopic assistance. Instruments in the CoC-NMR are supported in part by NIH S10OD024998. We also thank Z. Zhou at the QB3 Chemistry Mass Spectrometry Facility for her assistance with GC-MS measurements. SEM was conducted using facilities at the National Center for

Electron Microscopy and Imaging and Nanofabrication facilities at the Molecular Foundry. Work at the Molecular Foundry was supported by the Office of Science, Office of Basic Energy Sciences, of the US Department of Energy under Contract DE-AC02-05CH11231. We also thank Dr. Kyle Sander for assistance with *E. coli* growth experiments. S.C.-B. thanks the Philomathia Foundation for a personal fellowship.

AUTHOR CONTRIBUTIONS

S.C.-B. and S.L. contributed equally and have the right to list their name first in relevant applications. S.C-B. and S.L. designed and led the experiments. S.C.B., M.B.R., Y.L. and P.Y. conceived of the project. Y.L. assisted in CO_2 reduction experiments. T.C.D. helped with HPAEC-PAD work. J.N.C.S. facilitated MS protocol development. All authors wrote, discussed, and revised the manuscript.

COMPETING INTERESTS

Authors declare that they have no competing interests.

FIGURES

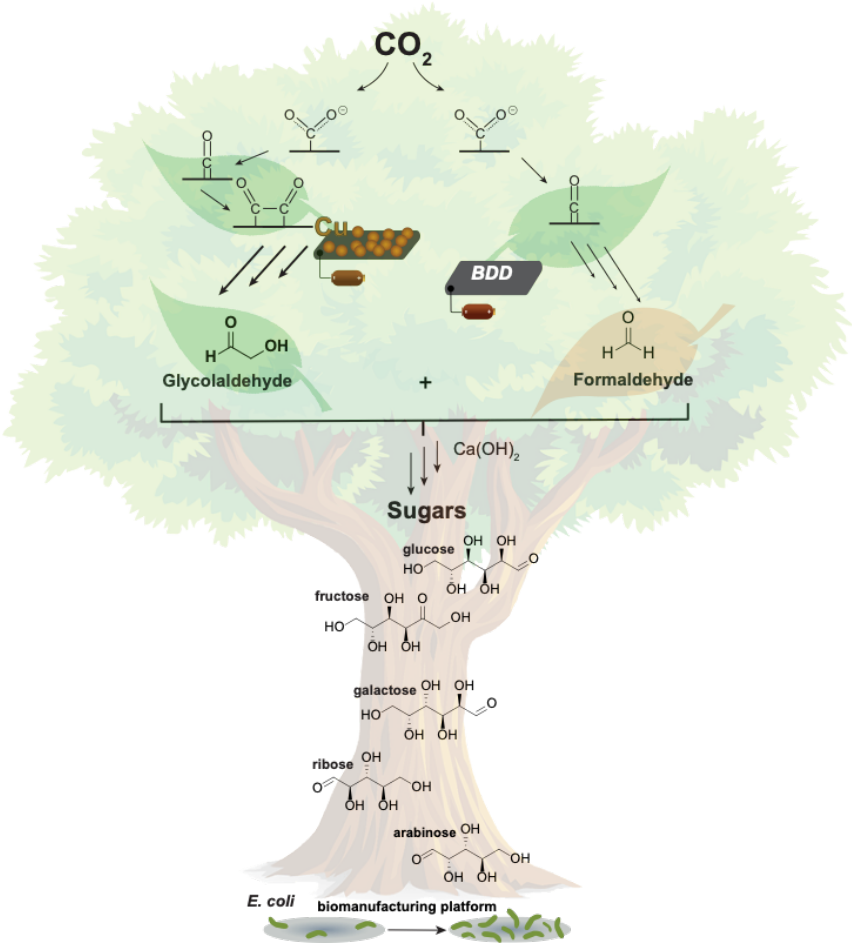

Figure 1 | Concept scheme: coupling of electrosynthesis with thermocatalysis to convert CO_2 to sugars. CO_2 is electrochemically reduced on copper nanoparticle and boron-doped diamond cathodes to glycolaldehyde and formaldehyde, respectively. The thermochemical conversion of formaldehyde with glycolaldehyde is initiated with a divalent metal cation (e.g., $Ca(OH)_2$) at mildly elevated temperatures (<100°C). The generated sugars are readily used as a feedstock for *Escherichia coli* enabling the quick conversion of CO_2 to a multitude of complex chemicals.

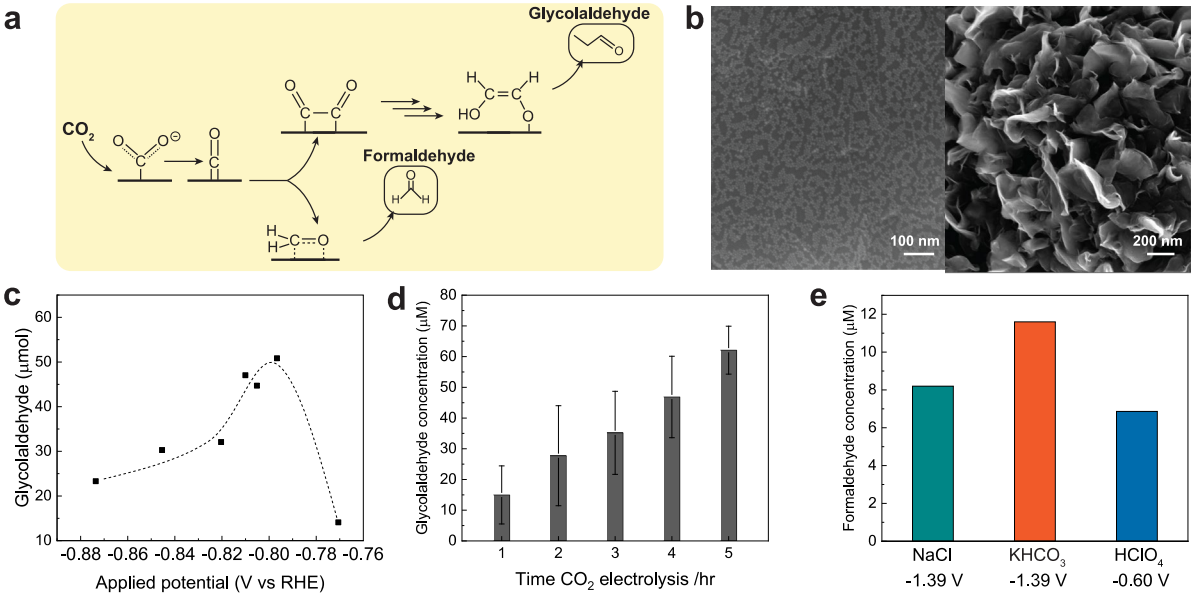

Figure 2 | CO_2 electrolysis produces upgradeable aldehydes. (a) Scheme of the mechanistic pathway of CO_2 electroreduction to glycolaldehyde and formaldehyde. **(b)** SEM of the Cu NP ensemble (left) and the BDD (right) electrocatalysts. **(c)** Concentration of glycolaldehyde obtained after 4 hours of CO_2 electrolysis in 0.1 M $KHCO_3$ using the Cu NP ensemble at various applied potentials. **(d)** Accumulation of glycolaldehyde produced at -0.80 V vs RHE as a function of electrolysis time using the Cu NP ensemble in 0.1 M $KHCO_3$. (e) Concentration of formaldehyde obtained after 1 hour of CO_2 electrolysis using a BDD electrode. All applied potentials are reported on the RHE scale. Error bars are one standard deviation of three independent measurements for the experimental data.

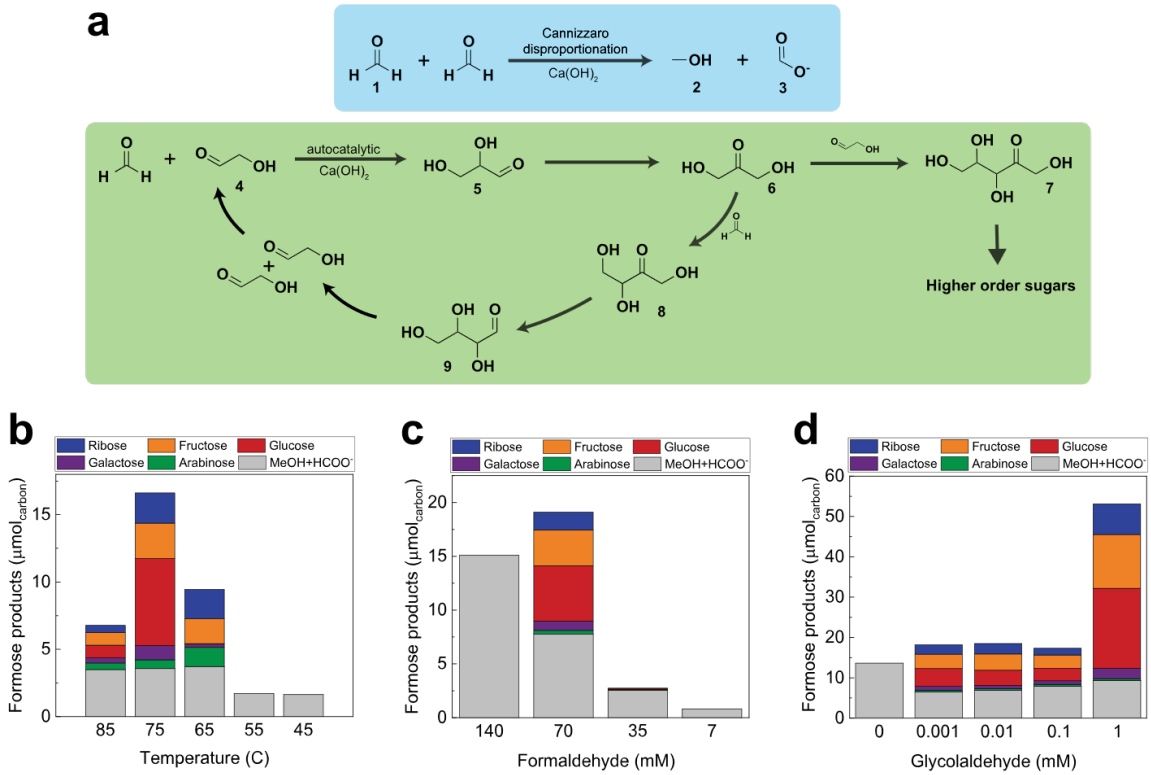

Figure 3 | Formose reaction overview and optimization. (a) Upper inset: the Cannizzaro disproportionation of formaldehyde (1) methanol (2) and formate (3). In the absence of glycolaldehyde as an autocatalyst, the Cannizzaro reaction dominates in alkaline and aqueous conditions. Lower inset: overview of the formose reaction autocatalyzed with glycolaldehyde (4). Briefly, an aldol condensation of (1) and (4) generates glyceraldehyde (5), which undergoes an aldose-ketose isomerization to make dihydroxyacetone (6). (6) and (4) react to form ribulose which isomerizes to ribose (7). (6) may also undergo a further aldol condensation with (1) to make tetrulose (8), which isomerizes to aldetrose (9). A retro-aldol reaction of (9) produces two molecules of (4), thus forming an autocatalytic cycle. **(b)**, **(c)** and **(d)** Formose reaction optimization based on temperature, formaldehyde, and glycolaldehyde concentrations, respectively. Biologically relevant products are quantified by HPAEC-PAD.

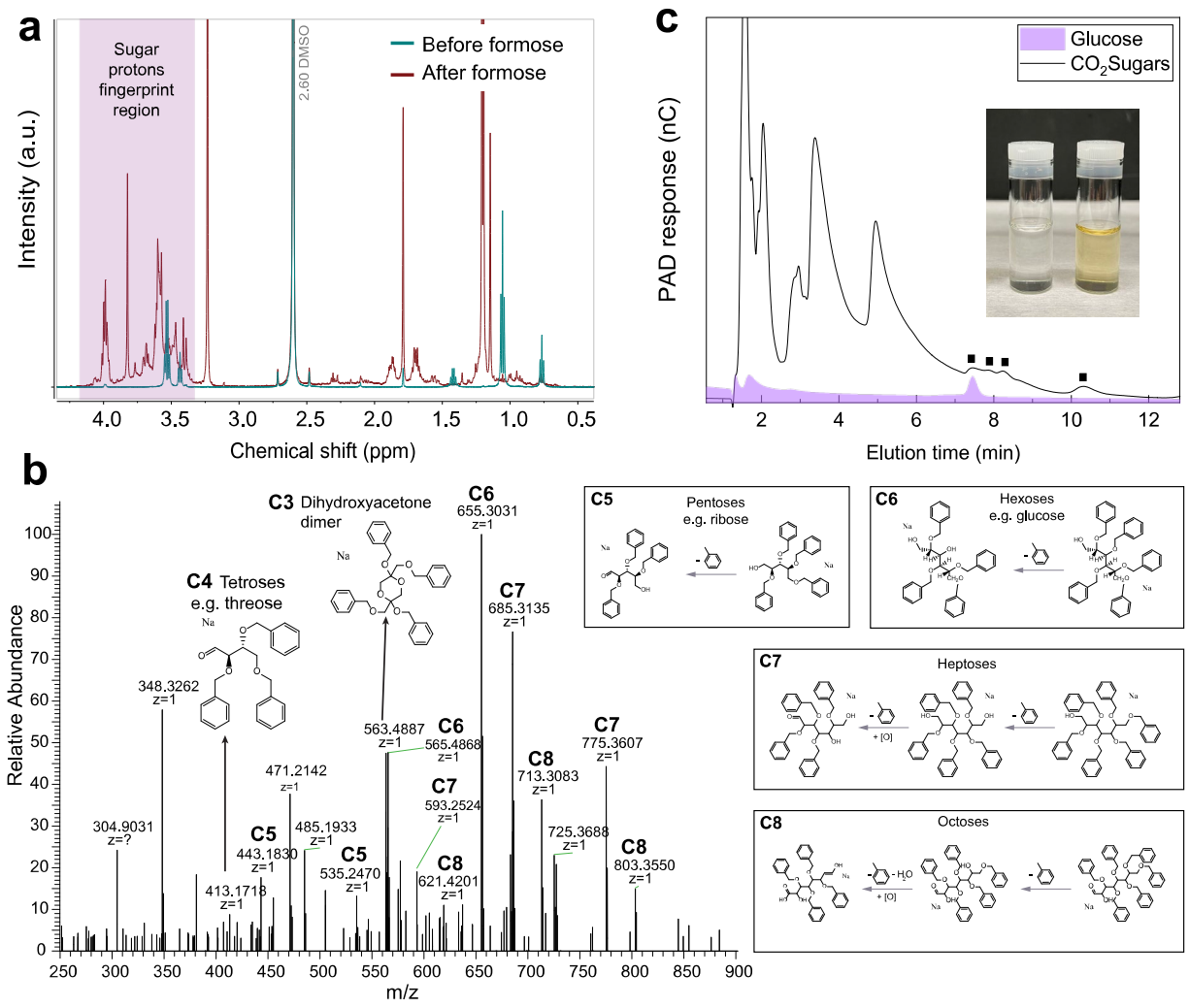

Figure 4 | Sugar synthesis catalyzed by CO_2 derived glycolaldehyde. (a) ^{1}H-NMR spectra pre- and post- formose reaction demonstrating the appearance of carbohydrate protons in the 3.5-5ppm region. **(b)** ESI-MS spectrum reveals a diverse mixture of benzylated sugars including pentoses, hexoses, heptoses, and octoses. **(c)** HPAEC-PAD spectrum reveals the presence of distinguishable CO_2Sugars obtained from the product stream of Cu NP ensemble at -0.80 V vs RHE. Visible peaks in the chromatograms are indicated by black squares. One of them is identified as glucose as it overlays closely with the glucose reference chromatogram. Inset picture displays the product of the formose reaction without e-CO_2Glyc (left) and autocatalyzed by e-CO_2Glyc (right). The yellow color is characteristic of sugar production.

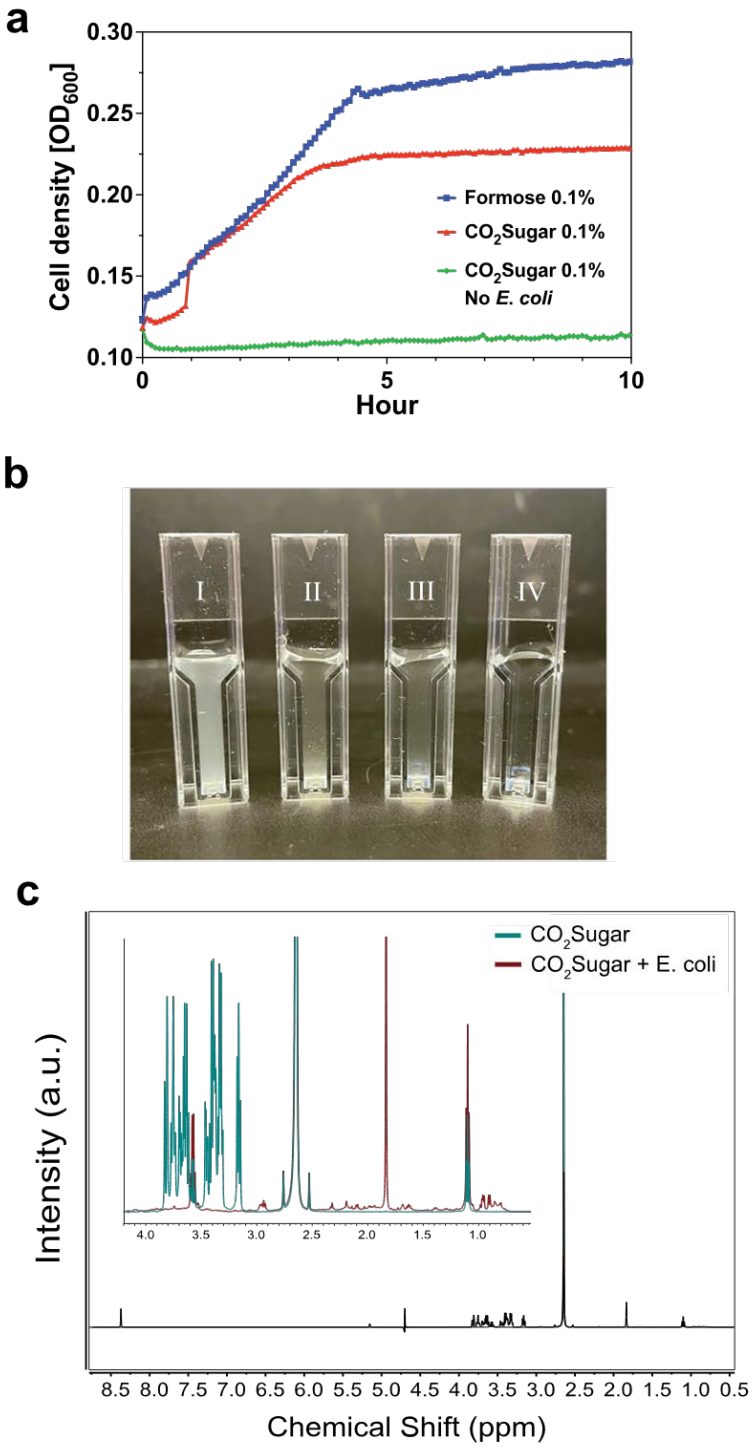

Figure 5 | Utilization of CO_2Sugar as a bacterial feedstock. (a) Optical density measurements of *Escherichia coli* (*E. coli*) cultured with formose sugars (blue) and CO_2Sugars (red). Control is CO_2Sugars without *E. coli* (green). **(b)** Picture comparing the visual differences between *E. coli* cultures provided with different sugars. From left to right: I. glucose, II. formose sugars, III. CO_2Sugars, and IV. CO_2Sugars without *E. coli*. **(c)** ^{1}H-NMR spectra of CO_2Sugar containing minimal medium pre- and post-*E. coli* culture growth. Inset shows magnified 1-4 ppm region.